tute (24) in (39) to obtain the field from the image. Noting that the integral contains a Fourier transformation of the Gaussian pulse, which has a known solution [8],

$$\int_{-\infty}^{\infty} e^{-jk_1\alpha\tau} e^{-\zeta^2/8\sigma^2}\, d\zeta = \sqrt{8\pi}\,\sigma e^{-2\sigma^2 k_1^2 \alpha^2}, \qquad (40)$$

we can write with $\alpha = \cos\theta_i$

$$\mathbf{E}^r(\mathbf{r}) \approx \mp e^{-2\sigma^2 k_1^2 \cos^2\theta_i} \left[-\nabla \times \left(\mathbf{u}_z M_0 L \frac{1}{4\pi r_1} e^{-jk_1 r_1} \right) \right]. \qquad (41)$$

This expression can be interpreted as follows. The term in square brackets is the far field from a vertical magnetic dipole at $z = -z_0$. The factor in front is the specular reflection coefficient $R_s = \mp 1$, and the Gaussian term in between equals that of (2), the effect of the rough surface. Thus, (41) can be interpreted through the ray theory and Fresnel reflection from the rough surface.

Similar considerations can be made for the more general source and medium cases, omitted here for conciseness.

4. CONCLUSION AND DISCUSSION

Image theory, previously developed for problems involving a smooth planar interface of two media, was extended to take into account a slight roughness of the interface. The analysis was based on the simple reflection coefficient expression corresponding to the coherent reflection field, for roughness obeying Gaussian statistics. The resulting image was seen to be the convolution of the specular image and a Gaussian pulse, which gives a blurred specular image.

The change in the amplitude of the coherent reflected wave due to the roughness of the surface can be easily interpreted in terms of the image theory. When a point image becomes a line image of Gaussian distribution, the ensuing phase differences causes partial cancellation in the radiated field. This effect is most notable in the normal direction and disappears in the direction tangential to the interface.

The image principle described in the article can be applied to a wide variety of problems involving a rough surface. For example, scattering from an object above a rough surface can be handled by replacing the object through an equivalent polarization source, which can be determined by replacing the material half space by the images of the original source and that of the unknown equivalent source. Limitations to the application of the theory are due to the simple starting point: the reflection coefficient expression requires that the source be sufficiently far from the interface and the roughness be slight enough.

REFERENCES

1. I. V. Lindell, "Application of the Image Concept in Electromagnetics," in W. R. Stone (Ed.), *URSI Review of Radio Science 1990–1992*, Oxford University Press, Oxford, 1993, pp. 107–126.
2. I. V. Lindell, *Methods for Electromagnetic Field Analysis* (2nd ed.), Oxford University Press, Oxford, 1995.
3. P. Beckmann and A. Spizzichino, *The Scattering of Electromagnetic Waves from Rough Surfaces*, Pergamon Press, Oxford, 1963.
4. J. A. DeSanto, *Scalar Wave Theory, Green's Functions and Applications*, Springer, Berlin, 1992, pp. 97–99.
5. I. V. Lindell, "Heaviside Operational Calculus in Electromagnetic Image Theory," *J. Electromagn. Waves Appl.*, to be published.
6. B. van der Pol and H. Bremmer, *Operational Calculus Based on the Two-Sided Laplace Integral* (2nd ed.), Cambridge University Press, 1959.
7. I. V. Lindell and E. Alanen, "Exact Image Theory for the Sommerfeld Half-Space Problem. Part I: Vertical Magnetic Dipole," *IEEE Trans. Antennas Propagat.*, Vol. AP-32, No. 2, 1984, pp. 126–133.
8. M. Abramowitz and I. Stegun, *Handbook of Mathematical Functions*, Dover, New York, 1966.

CCC 0895-2477/97

APPLICATION OF A POLE-FREE MODAL FIELD-MATCHING TECHNIQUE TO RIDGED RECTANGULAR WAVEGUIDES

Smain Amari[1] and Jens Bornemann[1]
[1] Laboratory for Lightwave Electronics, Microwaves and Communications LLiMiC
Department of Electrical and Computer Engineering
University of Victoria
Victoria, British Columbia, Canada V8W 3P6

Received 13 November 1996

ABSTRACT: *The poles in the determinantal equation of the standard modal field-matching technique (MFMT) are systematically eliminated, which results in well-behaved determinants. The pole-free characteristic matrix is shown to take a simple form. Excellent agreement between results from the present technique and previously published data is established. © 1997 John Wiley & Sons, Inc.* Microwave Opt Technol Lett 14: 337–340, 1997.

Key words: *ridged rectangular waveguide; field-matching technique; numerical methods*

I. INTRODUCTION

Eigenvalue problems in numerical modeling of electromagnetic phenomena are often reduced to a homogeneous matrix equation of the form

$$[A(k)][x] = 0. \qquad (1)$$

Here $[A(k)]$ is a parameter-dependent $n \times n$ matrix and $[x]$ is an unknown n-element vector [1, 2]. The parameter k often denotes the propagation constant, resonant frequency, or cutoff wave number. Nontrivial solutions to Eq. (1) are obtained when the matrix $[A(k)]$ becomes singular, or

$$\mathrm{Det}[A(k)] = 0, \qquad k = k_0 \qquad (2)$$

for a certain value k_0 of the parameter k.

The actual solution of Eq. (2) is often hindered by the presence of poles in the determinant of the characteristic matrix $[A(k)]$. The modal field-matching technique (MFMT) is a typical numerical method that suffers from these pathologies. Reliable computer codes can be developed only when these poles are recognized and efficiently handled.

Attempts at solving this problem are custom made and tailored to specific problems where the locations of the poles

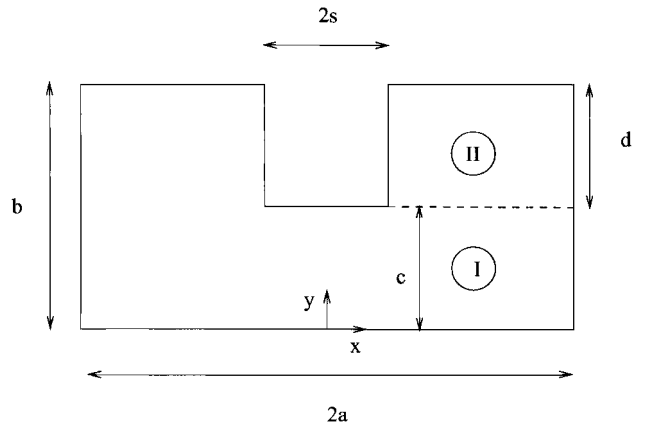

Figure 1 Cross section of a ridged rectangular waveguide and its subdivision for modal analysis

are determined in a first step to determine the zeros in the second step [3, 4]. The efficiency of such an approach is limited and requires extra CPU time to identify and eliminate the poles.

In this article we examine the origin of the poles in the determinantal equation within the MFMT. These numerical singularities are traced back to inversions of singular matrices in constructing the characteristic matrix $[A(k)]$. By carefully avoiding such operations, we show how to construct a pole-free characteristic matrix, thereby systematically eliminating the poles that appear in the standard MFMT.

II. CUTOFF WAVE-NUMBERS RIDGED RECTANGULAR WAVEGUIDE

The cross section of a ridged rectangular waveguide is shown in Figure 1. All metallic walls are assumed lossless.

Given the symmetry of the structure, its modes can be split into sets with magnetic and electric wall symmetries. Only TE modes with a magnetic wall are analyzed in detail here, although numerical results will be given for both symmetries.

The transverse components of the electromagnetic field of these modes can derived from its axial component H_z. The following expansions are used in the two subregions:

$$H_z^{\mathrm{I}}(x,y) = \sum_{n=1}^{\infty} A_n \cosh[\gamma_{1n} y] \sqrt{\frac{2}{a}} \sin\left[\frac{2n-1}{2}\pi\frac{x}{a}\right] \quad (3a)$$

and

$$H_z^{\mathrm{I}}(x,y) = \sum_{m=0}^{\infty} B_m \cosh[\gamma_{2m}(y-c-d)] \times \sqrt{\frac{2}{(a-s)(1+\delta_{m0})}} \cos\left[m\pi\frac{x-s}{a-s}\right]. \quad (3b)$$

Here

$$\gamma_{1n}^2 = \left(\frac{2n-1}{2a}\pi\right)^2 - k_c^2, \qquad \gamma_{2m} = \left(\frac{m\pi}{a-s}\right)^2 - k_c^2,$$

and k_c is the cutoff wave number.

At cutoff, the only E_x and E_y are nonvanishing, in addition to H_z. It is consequently sufficient to enforce the continuity of E_x and H_z at the interface I–II. The boundary conditions of the these modes can be written as

$$H_z^{\mathrm{I}}(x, y=c) = H_z^{\mathrm{II}}(x, y=c), \qquad s \le x \le a, \quad (4a)$$

$$E_x^{\mathrm{I}}(x, y=c) = 0, \qquad 0 \le x \le s, \quad (4b)$$

and

$$E_x^{\mathrm{I}}(x, y=c) = E_x^{\mathrm{II}}(x, y=c), \qquad s \le x \le a. \quad (4c)$$

In the standard MFMT, Eqs. (3) are used in Eqs. (4) to obtain two sets of linear and homogeneous equations in the expansion coefficients $[A]$ and $[B]$:

$$[A] = [C][B],$$
$$[B] = [D][A], \quad (5)$$

where

$$[C]_{nm} = -\frac{\gamma_{2m}\sinh[\gamma_{2m}d]}{\gamma_{1n}\sinh[\gamma_{1n}d]} \frac{2}{\sqrt{a(a-s)(1+\delta_{m0})}} \times \int_s^a \sin\left[\frac{(2n-1)\pi x}{2a}\right] \cos\left[m\pi\frac{x-s}{a-s}\right] dx = -\frac{\gamma_{2m}\sinh[\gamma_{2m}d]}{\gamma_{1n}\sinh[\gamma_{1n}c]}[L]_{nm} \quad (6a)$$

and

$$[D]_{nm} = \frac{\cosh[\gamma_{1m}c]}{\cosh[\gamma_{2n}c]} \frac{2}{\sqrt{a(a-s)(1+\delta_{n0})}} \times \int_s^a \sin\left[\frac{(2m-1)\pi x}{2a}\right] \cos\left[n\pi\frac{x-s}{a-s}\right] dx = \frac{\cosh[\gamma_{1m}c]}{\cosh[\gamma_{2n}d]}[L]_{mn}. \quad (6b)$$

If we eliminate $[A]$ from Eq. (5), for example, get

$$\{[D][C] - [U]\}[B] = 0, \quad (7)$$

where $[U]$ is the unit matrix. Nontrivial solutions to Eq. (7) exist only when

$$\mathrm{Det}\{[D][C] - [U]\} = 0. \quad (8)$$

The cutoff wave numbers of the structure are given by this determinantal equation. The actual determination of these cutoff wave numbers is, however, hindered by the presence of poles in the determinant in Eq. (8), as Figure 2(a) clearly shows. Even if one only searches for the sign changes in the determinant, the presence of the poles presents a real difficulty as the determinant changes sign in the vicinity of a pole, thereby introducing nonphysical roots.

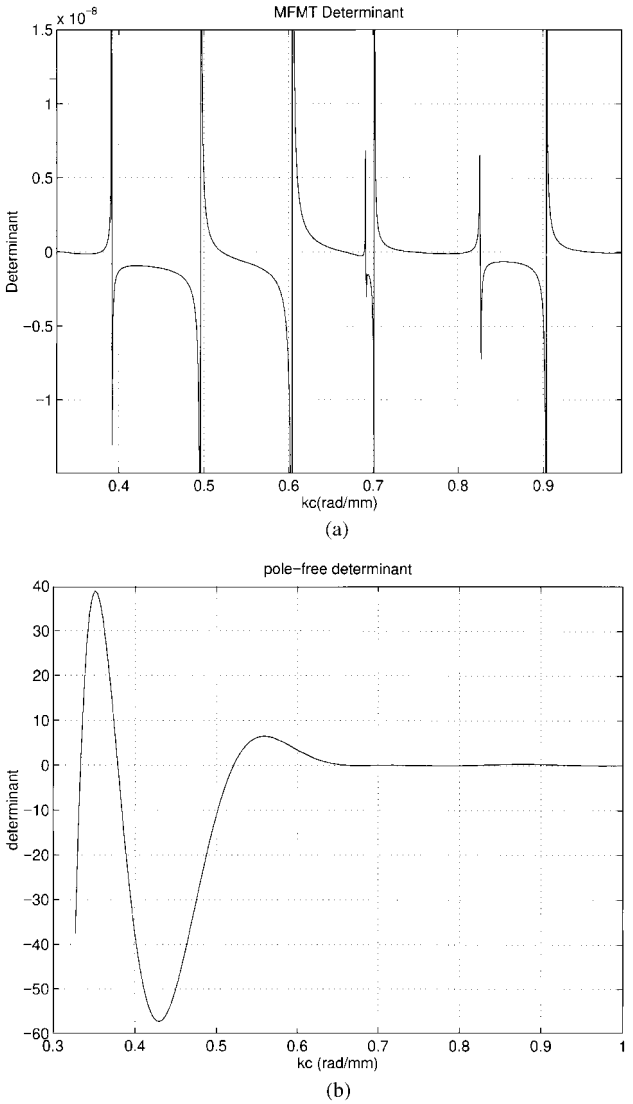

Figure 2 Determinant as a function of k_c (rad/mm) when $N = 3$. (a) Standard MFMT and (b) pole-free MFMT (this work)

To eliminate these poles, we have to identify their origin first. It is clear from the form of the matrices $[C]$ and $[D]$ that poles are present in the determinant whenever a denominator in either $[C]$ or $[D]$ vanishes. To avoid these singularities, we use expansions (3) in the boundary conditions (4) to get

$$[\text{diag}(\gamma_1 \sinh[\gamma_1 c])][A] = -[L][\text{diag}(\gamma_2 \sinh[\gamma_2 d])][B], \tag{9a}$$

and

$$[\text{diag}(\cosh[\gamma_2 d])][B] = [L]^T[\text{diag}(\cosh[\gamma_1 c])][A]. \tag{9b}$$

Here, $[\text{diag}(\gamma_1 \sinh[\gamma_1 c])]$, $[\text{diag}(\gamma_2 \sinh[\gamma_2 c])]$, $[\text{diag}(\cosh[\gamma_2 d])]$, and $[\text{diag}(\cosh[\gamma_1 c])]$ are diagonal matrices, and $[L]$ is defined in Eqs. (6).

Using Eq. (9b) in (9a), we get

$$\Big\{[L][\text{diag}(\gamma_2 \sinh[\gamma_2 d])][\text{diag}(\cosh[\gamma_2 d])]^{-1}[L]^T \times [\text{diag}(\cosh[\gamma_1 c])] + [\text{diag}(\gamma_1 \sinh[\gamma_1 c])]\Big\}[A] = 0. \tag{10}$$

In its present form, Eq. (10) contains the inverse of $[\text{diag}(\cosh[\gamma_2 d])]$, which introduces poles for some imaginary values of γ_2. We therefore multiply Eq. (10) from the left by $[L]^{-1}$ to get

$$\Big\{[\text{diag}(\cosh[\gamma_2 d])]^{-1}[\text{diag}(\gamma_2 \sin h[\gamma_2 d])][L]^T \times [\text{diag}(\cosh[\gamma_1 c])] + [L]^{-1}[\text{diag}(\gamma_1 \sinh[\gamma_1 c])]\Big\}[A] = 0. \tag{11}$$

Note that the order of the two diagonal matrices following $[L]$ in Eq. (10) was reversed, as two diagonal matrices always commute. Finally, by multiplying Eq. (11) from the left by $[\text{diag}(\cosh[\gamma_2 d])]$, we get a pole-free matrix equation:

$$\{[\text{diag}(\cosh[\gamma_2 d])][L]^{-1}[\text{diag}(\gamma_1 \sinh[\gamma_1 c])] + [\text{diag}(\gamma_2 \sinh[\gamma_2 d])][L]^T[\text{diag}(\cosh[\gamma_1 c])]\}[A] = 0. \tag{12}$$

The cutoff wave numbers are given by the roots of the determinant of the matrix $[K]$, given by

$$[K] = [\text{diag}(\cosh[\gamma_2 d])][L]^{-1}[\text{diag}(\gamma_1 \sinh[\gamma_1 c])] + [\text{diag}(\gamma_2 \sinh[\gamma_2 d])][L]^T[\text{diag}(\cosh[\gamma_1 c])]. \tag{13}$$

Note that the matrix $[K]$ involves diagonal matrices and takes the following simple form:

$$[K]_{mn} = \cosh[\gamma_{2m} d][L]^{-1}_{mn}\gamma_{1n} \sinh[\gamma_{1n} c] + \gamma_{2m} \sin h[\gamma_{2m} d][L]_{nm} \cosh[\gamma_{1n} c]. \tag{14}$$

The determinant of the matrix $[K]$ is pole free, as Figure 2(b) shows. Even though the matrix $[K]$ involves inverting the matrix $[L]$, this is done *only once* at the beginning of the search for the roots, as $[L]$ is independent of the wave number k_c.

TABLE 1 Cutoff Wave Numbers (rad / mm) of the First Eight TE Modes in a Single-Ridge Waveguide

Mode	1	2	3	4	5	6	7	8
Pole-free MFMT	0.0928	0.3332	0.3808	0.5260	0.6654	0.6911	0.7456	0.8290
Ref. [5]	0.0930	0.3332	0.3881	0.5265	0.6654	0.6913	0.7456	0.8298
Ref. [6]	0.0928	0.3332	0.3810	0.5262	0.6654	0.6912	0.7456	0.8294

$a = b = 9.5$ mm, $s = 0.15$ mm, $c = 1.7$ mm, $d = 7.8$ mm.

TABLE 2 Cutoff Wave Numbers (rad / mm) of the First Eight TM Modes in a Single-Ridge Waveguide

Mode	1	2	3	4	5	6	7	8
Pole-free MFMT	0.4711	0.4714	0.7411	0.7416	0.7477	0.7485	0.9396	0.9420
Ref. [5]	0.4665		0.7358					0.9427

$a = b = 9.5$ mm, $s = 0.15$ mm, $c = 1.7$ mm, $d = 7.8$ mm

III. NUMERICAL RESULTS

The present pole-free formulation of the modal field-matching technique (MFMT) is applied to determine the cutoff wave numbers of a ridged rectangular waveguide.

Table 1 gives the cutoff wave numbers k_c in rad/mm of the first eight TE modes with a magnetic wall symmetry. Our results agree well with those presented in References [5] and [6]. In computing these results, the sign of the determinant of the matrix $[K]$ in Eq. (14) was used, instead of its actual numerical value in conjunction with the bisection method. By using the sign of the determinant, overflows and underflows are avoided by proper scaling of the entries of the matrix $[K]$. Ten modes were found sufficient to achieve convergence.

Table 2 gives the cutoff wave numbers of the first eight TM modes. Both symmetries are included in this table. Note that some of the roots were not reported in Reference [5]. Good agreement is again observed between our result and the roots reported in [5].

IV. CONCLUSION

A pole-free formulation of the modal field-matching technique (MFMT) was applied to determine the spectrum of a ridged rectangular waveguide. The poles that plague the standard MFMT are *systematically* eliminated from the determinantal equation without requiring prior knowledge of their location or nature. Numerical results from the present formulation are in excellent agreement with previously published data.

REFERENCES

1. T. Itoh (Ed.), *Numerical Techniques for Microwave and Millimeter-Wave Passive Structures,* John Wiley & Sons, New York, 1989.
2. R. Sorrentino (Ed.), *Numerical Methods for Passive Microwave and Millimeter-Wave Structures*, IEEE Press, New York, 1989.
3. C. A. Olley and T. E. Rozzi, "Systematic Characterization of the Spectrum of Unilateral Finline," *IEEE Trans. Microwave Theory Tech.*, Vol. MTT-34, Nov. 1986, pp. 1147–1156.
4. A. S. Omar and K. Schunemann, "Pole-Free Formulation for the Determination of Finline Modes," *SBMO Int. Microwave Symp. Proc.*, Rio de Janeiro, Brazil, July 1987, pp. 477–481.
5. Y. Utsumi, "Variational Analysis of Ridged Wavguide Modes," *IEEE Trans. Microwave Theory Tech.*, Vol. MTT-32, Feb. 1985, pp. 111–120.
6. A. S. Omar and K. F. Schünemann, "Application of the Generalized Spectral-Domain Technique to the Analysis of Rectangular Waveguides with Rectangular and Circular Metallic Inserts," *IEEE Trans. Microwave Theory Tech.*, Vol. MTT-39, June 1991, pp. 944–952.

CCC 0895-2477/97

THE FDTD METHOD APPLIED TO THE STUDY OF FERRITES WITH A NEGATIVE EFFECTIVE PERMEABILITY: A NEW ALGORITHM

Ch. Melon,[1] Th. Monediere,[1] and F. Jecko[1]
[1] I.R.C.O.M.
U.R.A. au C.N.R.S. No. 356
Equipe "Electromagnétisme"
Faculté des Sciences
123 Avenue Albert Thomas
87060 Limoges Cedex, France

Received 25 September 1996; revised 15 November 1996

ABSTRACT: *Ferrites, which are used in many microwave devices as circulators or isolators, have complex geometries. When subjected to a magnetic field ferrites exhibit anisotropic and dispersive permeability. If this magnetic field is orthogonal to the direction of propagation the ferrite is characterized by an effective permeability μ_{eff} that can be either positive or negative. Many ferrite devices work in a frequency range where μ_{eff} is negative. The particular behavior of ferrite in this case is studied in this article with the use of the finite-difference–time-domain (FDTD) method. First phenomena are presented in a one-dimensional case; then a new two-dimensional FDTD algorithm is presented. © 1997 John Wiley & Sons, Inc.* Microwave Opt Technol Lett 14: 340–344, 1997.

Key words: *ferrite; effective permeability; finite-difference–time-domain*

I. INTRODUCTION

Many authors have applied the FDTD method to the study of a saturated ferrite medium [1–6]. They present results in a frequency range where the effective permeability of ferrite is positive. The behavior of the material is completely different when its effective permeability is negative [7]. In this article the propagation in ferrite when $\mu_{\text{eff}} < 0$ is studied by FDTD. Criteria for good discretization are defined for the first time. The reflection coefficient at an interface air ferrite is calculated in a 1D case. At last a new 2D FDTD algorithm is developed to study a ferrite with negative effective permeability. This algorithm is validated by computation of resonant frequencies and field patterns of a ferrite resonant device.

II. THE FERRITE MEDIUM — EFFECTIVE PERMEABILITY

The ferrite is an anisotropic and dispersive medium with a tensorial permeability $(\tilde{\mu})$. $(\tilde{\mu})$ depends on frequency and on the static magnetic field. In the harmonic domain $(\tilde{\mu})$ can be written for a lossless saturated ferrite [7, 8].

$$(\tilde{\mu}) = \mu_0 \begin{pmatrix} \mu & -jK & 0 \\ jK & \mu & 0 \\ 0 & 0 & 1 \end{pmatrix}, \qquad \text{with } \mu = 1 + \frac{\omega_0 \omega_M}{\omega_0^2 - \omega^2}, \tag{1}$$

$$K = -\frac{\omega \omega_M}{\omega_0^2 - \omega^2},$$